Combined Exposure to Multiwalled Carbon Nanotubes and Dibutyl Phthalates Aggravated Airway Inflammation in Rats

Suli He (hesuli0093@163.com)
Central China Normal University https://orcid.org/0000-0003-3612-9431
haiyan peng
CCNU: Central China Normal University
Min Wu
CCNU: Central China Normal University
Chao Yan
CCNU: Central China Normal University
Jian Wan
CCNU: Central China Normal University
xin ye
CCNU: Central China Normal University
Hongmao Zhang
CCNU: Central China Normal University
Shumao Ding
CCNU: Central China Normal University

Research Article

Keywords: Airway inflammation, Multi-walled carbon nanotubes, Dibutyl phthalate, Combined exposure, Asthma

Posted Date: August 29th, 2023

DOI: https://doi.org/10.21203/rs.3.rs-3284434/v1

Abstract

Previous work has shown that mice exposed to DBP-adsorbed onto MWCNTs, via tail vein injection, displayed black lesions in their lungs. To investigate the mechanism causing this toxicity in the lung tissue of rats, we performed an experiment with SD rats, exposing them to DBP adsorbed onto MWCNTs via a tail vein injection for 14 days. The results revealed pulmonary edema and greyish-black lung tissue in the MWCNTs and the MWCNTs + DBP combined exposure groups. In the combined exposure group there was evident alveolar fragmentation and adhesion, and lung tissue sections showed significant levels of black particles. Sections of the non-cartilaginous region of the trachea had significant folding of the pseudostratified ciliated columnar epithelium and marked thickening of the submucosa. In BALF, the number of WBC, Lym, Neu, and Eos cells, as well as levels of IgE, IL-6, TNF-α, and IL-1β, were all significantly higher. TNF-α, IL-6, STAT3, and α-SMA mRNA expression were all elevated in the lung tissue. The combined exposure group, which had considerable airway remodeling, had a greater degree of tracheal constriction and luminal narrowing, according to the results of the α-SMA immunofluorescence assay. According to these experimental findings, the exposure to both MWCNTs and DBP seemed to have a synergistic effect and exacerbated rats' impaired respiratory function that resulted from exposure to MWCNTs alone.

1 Introduction

There is widespread pollution of multi-walled carbon nanotubes (MWCNTs) and dibutyl phthalate (DBP), and increasing evidence showing a link between exposure to MWCNTs or DBP and respiratory and allergic disease (Baralić et al., 2021; Ihrie et al., 2021). MWCNTs dripped into mice lungs, were shown to significantly increase pre-existing allergic airway inflammation in the mice, by encouraging the creation of cysteinyl leukotrienes (Carvalho et al., 2018). When exposed to NM-403, a type of MWCNTs, for four consecutive weeks, Sprague Dawley rats (SD rats) experienced acute lung inflammation and proliferative lung alterations (Barthel et al., 2023). Similarly, DBP exposure significantly increased airway inflammation and aggravated mice's allergic asthma brought on by OVA (Li et al., 2023). Unfortunately, the studies mentioned above have only focused on the respiratory effects of exposure to MWCNTs or DBP alone, and very few studies have focused on the consequences of simultaneous exposure to these pollutants, even though both MWCNTs and DBP are virtually always present in the living environment. According to our prior research, inflammation is triggered and oxidative stress is disrupted when MWCNTs and DBP are administered simultaneously to mice via tail vein injection, resulting in reproductive toxicity, immunotoxicity, and neurotoxicity (Ye et al., 2022; Zhou et al., 2022b; Zhou et al., 2022a). Such toxic effects were more severe than when mice were exposed to MWCNTs or DBP alone. Furthermore, lung autopsies showed that the lungs of the mice co-exposed to MWCNTs and DBP were all greyish-black in color. This phenomenon may be caused by the deposition of MWCNTs in the lungs. It was not known what negative effects the deposition of MWCNTs in lung tissue and the airways during this exposure would have, nor whether the presence of DBP would exacerbate these effects. To further our understanding of the potential risks from combined exposure on the respiratory system, we exposed

male SD rats to MWCNTs and DBP via a tail vein injection over 14 days. We aimed to examine the effects on both airways and lung tissue and to investigate the potential mechanisms responsible for these effects.

2 Materials and methods

2.1 Main experimental drugs

DBP (> 99%, CAS: 84-74-2) was purchased from Sigma-Aldrich, U.S.A. MWCNTs (> 95%, CAS: 308068-56-6, outer diameter < 8 nm, length 0.5-2 μm) were purchased from Shanghai Aladdin Biochemical Technology Co., Ltd (File 1).

2.2 Experimental animals

We purchased 40 5-week-old male SD rats from the Experimental Animal Management Division of the Hubei Provincial Disease Prevention and Control Center. The rats were acclimatized for 7 days in pathogen-free cages at 20–25°C and 50–70% relative humidity with a 12 h light-dark cycle.

2.3 Test methods

2.3.1 Grouping of experimental animals and exposure protocols

The 40 healthy male SD rats were randomly divided into four groups (10 per group): (1) Saline control group (control); (2) MWCNTs group (10 mg/kg/day); (3) DBP group (2.15 mg/kg/day); and (4) MWCNTs + DBP combined exposure group (10 mg/kg/day MWCNTs and 2.15 mg/kg/day DBP). The group was exposed every two days via tail vein injection, the exposure solution was ultrasonically shaken for 30 min before each injection. The DBP dose, 2.15 mg/kg, was chosen because it was the highest concentration that could be adsorbed onto the MWCNTs.

2.3.2 Gross observation of lung tissue

After the final exposure, the mice were anesthetized, and the chest opened to remove the entire lung, and adjacent organs and tissues. Filter paper was used to remove any blood from the surface of the lung tissue. The lung's aspect was then assessed and photographs were taken.

2.3.3 Lung tissue organ coefficient

The trachea was severed at 3mm from the tracheal fork. Blood and water were absorbed with filter paper, and the lungs were weighed to obtain the wet weight. The lung coefficient was then calculated as Lung coefficient = lung wet weight (g) / body weight (Kg).

2.3.4 Pathological analysis of lung tissue and trachea

The trachea and lung tissues of rats were separated and histopathological sections were prepared. All samples were incubated in 4% paraformaldehyde fixation solution for 24 hours at room temperature, distal portions were embedded in paraffin and sliced into 10 mm sections. These were stained with hematoxylin and eosin (H&E) according to standard protocols and observed using an inverted microscope (NIKOU-TE2000U, Tokyo, Japan).

2.3.5 Broncho alveolar lavage fluid (BALF) collection and cell counts

A 15G tracheal cannula with an inner diameter of 1.60 mm and an outer diameter of 1.8 mm was used to inject 2 mL of sterile saline slowly into the lungs of rats. After the 30s, this fluid was sucked out and set aside. This procedure was repeated three times (recovery rate > 75%). The recovered lavage fluid was centrifuged at 3000 r/min for 10 min at 4°C, and the supernatant was stored at -80°C for later examination. The residual cell mass was resuspended with 0.5 mL of sterile pre-cooled physiological saline, and an XN-1000V Automatic Cell Counter (Sysmex, Kobe, Japan) was used to analyze the type and number of cells in the BALF.

2.3.6 Determination of inflammatory factors and immunoglobulin E (IgE) in BALF

ELISA kits (Mlbio, Shanghai, China) were used to determine levels of TNF-α, IL-1β, IL-6, and IgE in the supernatant of the BALF.

2.3.7 RNA extraction and real-time quantitative polymerase chain reaction (RT-qPCR)

Total RNA from the rats' lung tissues was extracted using an ultrapure RNA extraction kit (Cwbio, Jiangsu, China), and then cDNA was synthesized using a reverse transcription kit (Accurate Biology, Hunan, China). The SYBR Green system (Accurate Biology, Hunan, China) and the CFX Connect Real-Time PCR Detection System (BIO-RAD, Singapore) were used for our real-time quantitative PCR analysis. All RT-qPCR expression assays were performed and analyzed at least three times in independent experiments. Transcript levels of β-actin were identified as housekeeping genes. The Ct values obtained were calculated and analyzed using the $2^{-\Delta\Delta CT}$ method (Livak and Schmittgen, 2001). Primer sequences for related genes are shown in Table 1.

Table 1
The Sequences of Gene Primers

Gene	Forward	Reverse
TNF-α	CCACGCTCTTCTGTCTACTG	GCTACGGGCTTGTCACTC
IL-6	ATTGTATGAACAGCGATGATGCAC	CCAGGTAGAAACGGAACTCCAGA
STAT3	GGGTCACTTTCACTTGGG	GGAATGTCAGGGTAGAGGTA
α-SMA	CCCACTGATACGCCTGAG	TGAAGCGAAAGCCCTGTA
β-actin	GCCCCTCTGAACCCTAA	GAGGCATACAGGGACAACA

2.3.8 Immunofluorescence detection of α-SMA expression in lung tissue

Paraffin sections of lung tissue were routinely deparaffinized, rehydrated, antigenically repaired, incubated, and closed, and then immunofluorescence stained with an anti-α-SMA antibody. After immunofluorescence staining, images were scanned, photographed, and analyzed with the aid of a laser confocal microscope (Leica-SP8, Germany). Quantitative analysis was performed using Image J software (NIH, Bethesda, MD, USA), in which images of six fields of view were randomly acquired, and then images to be quantified were converted to greyscale and the tissue regions of interest were circled. When applying Image J measurements, measurement units such as area and average grey scale were used to analyze the average fluorescence intensity of the region of interest.

2.4 Statistical processing

The experimental data were analyzed by one-way ANOVA using GraphPad Prism 7.0 software, the data graphs were automatically generated, and the experimental data were expressed as Mean ± SEM. $p < 0.05$ means there is a significant difference, which is indicated by "*", and when $p < 0.01$ is indicated by "**".

3 Results

3.1 Lung tissue organ coefficient

The lung tissue organ coefficient is an indicator of the degree of pulmonary oedema. As shown in Fig. 1, the lung tissue organ coefficient was significantly higher ($p < 0.05$) in the rats in the MWCNTs + DBP combined exposure group compared with the control group.

3.2 Histopathological analysis of lung tissue

3.2.1 Gross observation of lung tissue

Figure 2 provides a comprehensive illustration of the lungs. Rats in the control group (Fig. 2A) had rosy-pink, elastic, and lustrous lung tissues with no traces of gray or black buildup. The lung tissues of the mice in each of the exposure groups (Figs. 2B, 2C, and 2D) had decreased elasticity overall, with the lung tissues of the MWCNTs and MWCNTs + DBP groups exhibiting a grey to black color. The black material, which is the particulate deposition of MWCNTs, could be seen distributed in the interstitial spaces.

3.2.2 Morphological changes revealed by H&E staining of the trachea and lung tissue

Figure 3 shows a transverse section of the non-chondral area of the trachea. Compared with the control group (Fig. 3A), obvious folds of pseudo-complex ciliated columnar epithelium, hyperplasia of cup-shaped cells, and obvious thickening of the submucosal layer could be seen in the three exposure groups (Figs. 3B, 3C, and 3D).

Alveolar fragmentation and adhesion are visible in the lung tissue sections from the MWCNTs, DBP, and combined exposure groups compared to the control group, as shown in Fig. 4. All exposure groups showed some degree of lung parenchymalization, pink mucus, and a tiny amount of bleeding that could be seen in the alveolar lumen, with the DBP and combined exposure groups exhibiting most of these changes. Additionally, both the MWCNTs group and the combined exposure group showed lung macrophages that were black in color, with the combined exposure group having the greatest concentration of black particles.

3.3 Cytology of BALF

The results of cell counting in BALF are shown in Fig. 5. Compared with the control group, the numbers of WBC, Lym, Neu, and Eos cells in the MWCNTs + DBP combined exposure group were significantly increased ($p < 0.01$). The numbers of WBC and Lym in the combined exposure group were significantly higher than those in the DBP and MWCNTs groups, showing the synergistic effect of the combined exposure.

3.4 Levels of inflammatory factors and IgE in BALF

As shown in Fig. 6, the levels of TNF-α, IL-1β, IL-6, and IgE were significantly higher in the MWCNTs + DBP combined exposure group compared with the control group ($p < 0.01$), indicating that combined exposure had a strong sensitizing effect on rats.

3.5 Effect of combined exposure to MWCNTs and DBP on the expression of airway inflammatory marker genes in rats

As shown in Fig. 8, the mRNA expression of TNF-α, IL-6, STAT3, and α-SMA were significantly higher in the MWCNTs + DBP combined exposure group compared with the control group ($p < 0.01$). The expression

of TNF-α, IL-6, and STAT3 in the combined exposure group were significantly higher than that in the DBP and MWCNTs groups, indicating that there is a synergistic effect with combined exposure.

3.7 α-SMA immunofluorescence detection

Figure 8A illustrates the degree of bronchoconstriction and lumen narrowing in the various groups. This was significantly greater in the MWCNTs + DBP combined exposure group compared to the control group (DAPI staining). Airway smooth muscle (ASM) plays an important role in bronchoconstriction of the airways. Quantified α-SMA fluorescence staining of bronchial tubes in the lung sections (Fig. 8B) show that α-SMA expression increased in rats after MWCNTs + DBP exposure, and the fluorescence intensity was significantly higher than that in the control.

Figure 8A: Representative images of bronchia after immunofluorescence staining, scale bar 100 um; B: Quantification of α-SMA expression levels. The histogram values represent the Mean ± SEM (n = 10). * $p < 0.05$, ** $p < 0.01$.

4 Discussion

The unique tubular structure of MWCNTs allows for efficient loading and delivery of drugs, and are administered via intravenous injection in these cases (Xu et al., 2016). However, the biosafety of MWCNTs is of concern (Johnston et al., 2010; Chetyrkina et al., 2022). One study found that after mice were given 200 μg MWCNTs (containing radioactive salts) via tail vein injection, high levels of these were detected in the lungs (Gajewska et al., 2021). In this study, we found that lung macrophages in the MWCNTs and the combined exposure groups, phagocytosed MWCNTs in large numbers, resulting in lungs that were largely greyish-black in color. We used H&E staining to look for pathological changes in the airways and lung tissue and found different degrees of pathological changes in the trachea and lung tissues of the rats in the exposure groups compared to the control group. The lungs of rats in the combined exposure group showed extensive airway remodeling (tracheal constriction and lumen narrowing). Airway constriction is the main physiological event in asthma, and when an asthma attack occurs, the ASM constricts, narrowing the airways (Kudo et al., 2013; Hogg, 1997). Studies have shown that α-SMA can act directly on ASM, and overexpression of α-SMA can cause a series of changes in ASM such as airway constriction, lumen narrowing, and migration, thereby exacerbating airway inflammation and airway remodeling (Goldsmith et al., 2007; Hillsley et al., 2021). The results from our experiment showed that combined exposure to MWCNTs and DBP led to a significant increase in α-SMA expression, which is consistent with the findings of Wei et al., that lung inflammation is often accompanied by elevated α-SMA levels (Wei et al., 2023; Baek et al., 2021).

ASM is responsible for airway narrowing and is an important source of inflammatory mediators (Koopmans et al., 2020; Kume et al., 2023). Research has shown that activation of ASM cells by TNF-α or IL-1β induces the production of the pleiotropic cytokine IL-6 in ASM (Hirst, 2003; Fujita et al., 2011). IL-6 regulates a variety of inflammatory responses, including acute phase protein (APPs) production, B-cell

maturation, IgE up-regulation, and T-cell activation and differentiation, and these responses play a key role in the immune inflammatory response (Kamimura et al., 2003; Kang and Kishimoto, 2021). Our results showed that the gene levels and protein content of TNF-α, IL-1β, and IL-6 increased in the combined exposure group, and were significantly higher than those in the separate exposure groups. The increased production of inflammatory factors would lead to infiltration activation of eosinophils and overproduction of IgE (Nagata et al., 2020), which is consistent with our findings. Our results consistently suggest that combined exposure to MWCNTs and DBP will lead to severe immune imbalance. Oxidative damage is an important mechanism by which environmental pollutants induce airway inflammation (Pardo et al., 2020; Liu et al., 2023), and we did observe that significant oxidative damage occurred in the blood of rats exposed to MWCNTs and DBP (Figure S1). We, therefore, conclude that MWCNTs and DBP may synergistically increase airway inflammation in rats, leading to the pathophysiological changes associated with asthma.

Dysregulation of signaling pathways is implicated in the development of inflammation (Yeung et al., 2018). IL-6, a key cytokine involved in controlling inflammatory responses, either directly or indirectly activates STAT3, and activated STAT3 encourages the expression of inflammatory factors like IL-6, IL-1β, and IFN-γ and TNF-α by controlling gene transcription. Excessive levels of inflammatory factors trigger STAT3 phosphorylation, which thus increases the inflammatory response (Uciechowski and Dempke, 2020; Yousef et al., 2023). The results of our study showed that mRNA expression of TNF-α, IL-6, and STAT3 was significantly elevated in the MWCNTs + DBP combined exposure group, suggesting that this inflammatory signaling pathway may have been activated.

The interactions between co-existing pollutants and their resulting combined toxicity is a research frontier in environmental toxicology (Svadlakova et al., 2022; Wang et al., 2023). MWCNTs have been shown to adsorb DBP through π-π interactions, and thus form complexes in the environment (Wang et al., 2010). We showed, in this study, that the consequences of exposure to combined MWCNTs and DBP were significantly worse than for exposure to either alone, suggesting a possible synergistic effect, which is consistent with our previous studies (Zhou et al., 2022b; Qin et al., 2023). Based on this, we hypothesized that DBP adsorption on MWCNTs may operate as an "umbrella" to postpone the breakdown of DBP and so allow its transfer to a wider range of tissues and organs, leading to more severe endocrine-disrupting effects. Our experimental results revealed that activation of IL-6 and STAT3 in the combined exposure group was significantly higher than for either of the other exposure groups. This is most likely the result of MWCNTS and DBP binding to various sites on IL-6 or STAT3 thus promoting their activation, and having a cumulative effect on the activation of both these molecules. The specific mechanism needs further investigation.

5 Conclusion

The findings of this study indicate that combined exposure to MWCNTs and DBP could, in rats, synergistically exacerbate airway inflammation and promote airway remodeling, which further compromised lung function that ultimately results in the development of allergic asthma. These findings

suggest that we should pay more attention to the health effects of interactions between various environmental pollutants in the future.

CRedit authors statement: Suli He: Investigation; Methodology; Data curation; Visualization; Writing-original draft; Writing-review & editing. Haiyan Peng: Investigation; Methodology; Data curation; Visualization. Min Wu: Resources; Investigation; Methodology; Data curation. Chao Yan: Investigation; Methodology; Writing - editing. Jian Wan: Methodology; Data curation. Xin Ye: Investigation; Methodology. Hongmao Zhang: Methodology; Supervision; Writing-original draft; Writing-review & editing. Shumao Ding: Methodology; Supervision; Writing-original draft; Writing-review & editing.

Institutional Review Board Statement: The present study was designed to minimize the animal suffering and use amount according to the National Institutes of Health Guidelines in China, which was also permitted by the Animal Ethics Committee of Central China Normal University University College of Life Sciences (Permit number: CCNU-IACUC-2020-008). Also, the study was performed in compliance with the ARRIVE guidelines.

Declarations

Informed Consent Statement: Not applicable.

Declaration of competing interest: The authors declare that they have no known competing financial interests or personal relationships that could have appeared to influence the work reported in this paper.

Acknowledgments: This research was funded by the National Natural Science Foundation of China (General Program) (No. 32170508,31772471), and the Fundamental Research Funds for the Central Universities (No. CCNU22LJ003).

References

1. Baek H, Jang S, Park J, et al. (2021) Reduced receptor for advanced glycation end products is associated with α-SMA expression in patients with idiopathic pulmonary fibrosis and mice. *Laboratory Animal Research* 37(1): 28.
2. Baralić K, Bozic D, Živančević K, et al. (2021) Integrating in silico with in vivo approach to investigate phthalate and bisphenol A mixture-linked asthma development: Positive probiotic intervention. *Food and Chemical Toxicology* 158: 112671.
3. Barthel H, Sébillaud S, Lorcin M, et al. (2023) Needlelike, short and thin multi-walled carbon nanotubes: comparison of effects on wild type and p53(+/-) rat lungs. *Nanotoxicology* 17(3): 270-288.
4. Carvalho S, Ferrini M, Herritt L, et al. (2018) Multi-Walled Carbon Nanotubes Augment Allergic Airway Eosinophilic Inflammation by Promoting Cysteinyl Leukotriene Production. *Front Pharmacol* 9: 585.

5. Chetyrkina MR, Fedorov FS and Nasibulin AG (2022) In vitro toxicity of carbon nanotubes: a systematic review. *RSC Advances* 12(25): 16235-16256.
6. Fujita H, Chalubinski M, Rhyner C, et al. (2011) Claudin-1 expression in airway smooth muscle exacerbates airway remodeling in asthmatic subjects. *J Allergy Clin Immunol* 127(6): 1612-1621.e1618.
7. Gajewska A, Wang JT, Klippstein R, et al. (2021) Functionalization of filled radioactive multi-walled carbon nanocapsules by arylation reaction for in vivo delivery of radio-therapy. *J Mater Chem B* 10(1): 47-56.
8. Goldsmith AM, Hershenson MB, Wolbert MP, et al. (2007) Regulation of airway smooth muscle alpha-actin expression by glucocorticoids. *Am J Physiol Lung Cell Mol Physiol* 292(1): L99-l106.
9. Hillsley A, Santos JE and Rosales AM (2021) A deep learning approach to identify and segment alpha-smooth muscle actin stress fiber positive cells. *Scientific Reports* 11(1): 21855.
10. Hirst SJ (2003) Regulation of airway smooth muscle cell immunomodulatory function: role in asthma. *Respir Physiol Neurobiol* 137(2-3): 309-326.
11. Hogg JC (1997) The pathology of asthma. *Apmis* 105(10): 735-745.
12. Ihrie MD, Duke KS, Shipkowski KA, et al. (2021) STAT6-Dependent Exacerbation of House Dust Mite-Induced Allergic Airway Disease in Mice by Multi-Walled Carbon Nanotubes. *NanoImpact* 22.
13. Johnston HJ, Hutchison GR, Christensen FM, et al. (2010) A critical review of the biological mechanisms underlying the in vivo and in vitro toxicity of carbon nanotubes: The contribution of physico-chemical characteristics. *Nanotoxicology* 4(2): 207-246.
14. Kamimura D, Ishihara K and Hirano T (2003) IL-6 signal transduction and its physiological roles: the signal orchestration model. *Rev Physiol Biochem Pharmacol* 149: 1-38.
15. Kang S and Kishimoto T (2021) Interplay between interleukin-6 signaling and the vascular endothelium in cytokine storms. *Experimental & Molecular Medicine* 53(7): 1116-1123.
16. Koopmans T, Hesse L, Nawijn MC, et al. (2020) Smooth-muscle-derived WNT5A augments allergen-induced airway remodelling and Th2 type inflammation. *Scientific Reports* 10(1): 6754.
17. Kudo M, Ishigatsubo Y and Aoki I (2013) Pathology of asthma. *Front Microbiol* 4: 263.
18. Kume H, Yamada R, Sato Y, et al. (2023) Airway Smooth Muscle Regulated by Oxidative Stress in COPD. *Antioxidants (Basel)* 12(1).
19. Li Y, Yan B, Wu Y, et al. (2023) Ferroptosis participates in dibutyl phthalate-aggravated allergic asthma in ovalbumin-sensitized mice. *Ecotoxicol Environ Saf* 256: 114848.
20. Liu X, Pan B, Wang X, et al. (2023) Ischemia/reperfusion-activated ferroptosis in the early stage triggers excessive inflammation to aggregate lung injury in rats. *Front Med (Lausanne)* 10: 1181286.
21. Livak KJ and Schmittgen TD (2001) Analysis of relative gene expression data using real-time quantitative PCR and the 2(-Delta Delta C(T)) Method. *Methods* 25(4): 402-408.
22. Nagata M, Nakagome K and Soma T (2020) Mechanisms of eosinophilic inflammation. *Asia Pac Allergy* 10(2): e14.

23. Pardo M, Qiu X, Zimmermann R, et al. (2020) Particulate Matter Toxicity Is Nrf2 and Mitochondria Dependent: The Roles of Metals and Polycyclic Aromatic Hydrocarbons. *Chem Res Toxicol* 33(5): 1110-1120.
24. Qin Y, He S, Peng H, et al. (2023) Dibutyl Phthalate Adsorbed on Multiwalled Carbon Nanotubes Causes Fetal Developmental Toxicity in Balb/C Mice. 11(7): 565.
25. Svadlakova T, Holmannova D, Kolackova M, et al. (2022) Immunotoxicity of Carbon-Based Nanomaterials, Starring Phagocytes. *Int J Mol Sci* 23(16).
26. Uciechowski P and Dempke WCM (2020) Interleukin-6: A Masterplayer in the Cytokine Network. *Oncology* 98(3): 131-137.
27. Wang F, Yao J, Sun K, et al. (2010) Adsorption of dialkyl phthalate esters on carbon nanotubes. *Environ Sci Technol* 44(18): 6985-6991.
28. Wang Z, Ma J, Wang T, et al. (2023) Environmental health risks induced by interaction between phthalic acid esters (PAEs) and biological macromolecules: A review. *Chemosphere* 328: 138578.
29. Wei L, Hongping H, Chufang L, et al. (2023) Effects of Shiwei Longdanhua formula on LPS induced airway mucus hypersecretion, cough hypersensitivity, oxidative stress and pulmonary inflammation. *Biomed Pharmacother* 163: 114793.
30. Xu YY, Ge J, Zhang MH, et al. (2016) Intravenous Administration of Multiwalled Carbon Nanotubes Aggravates High-Fat Diet-Induced Nonalcoholic Steatohepatitis in Sprague Dawley Rats. *Int J Toxicol* 35(6): 634-643.
31. Ye X, Zhou T, Qin Y, et al. (2022) Reproductive toxicity of dibutyl phthalate adsorbed on carbon nanotubes in male Balb/C mice. *Reprod Toxicol* 110: 180-187.
32. Yeung YT, Aziz F, Guerrero-Castilla A, et al. (2018) Signaling Pathways in Inflammation and Anti-inflammatory Therapies. *Curr Pharm Des* 24(14): 1449-1484.
33. Yousef EH, El-Magd NFA and El Gayar AM (2023) Norcantharidin potentiates sorafenib antitumor activity in hepatocellular carcinoma rat model through inhibiting IL-6/STAT3 pathway. *Transl Res*. Epub ahead of print 2023/06/01. DOI: 10.1016/j.trsl.2023.05.005.
34. Zhou T, He S, Ye X, et al. (2022a) Exposure to dibutyl phthalate adsorbed to multi-walled carbon nanotubes causes neurotoxicity in mice by inducing the release of BDNF. *Science of The Total Environment* 852: 158319.
35. Zhou T, He Y, Qin Y, et al. (2022b) Exposure to a combination of MWCNTs and DBP causes splenic toxicity in mice. *Toxicology* 465: 153057.

Figures

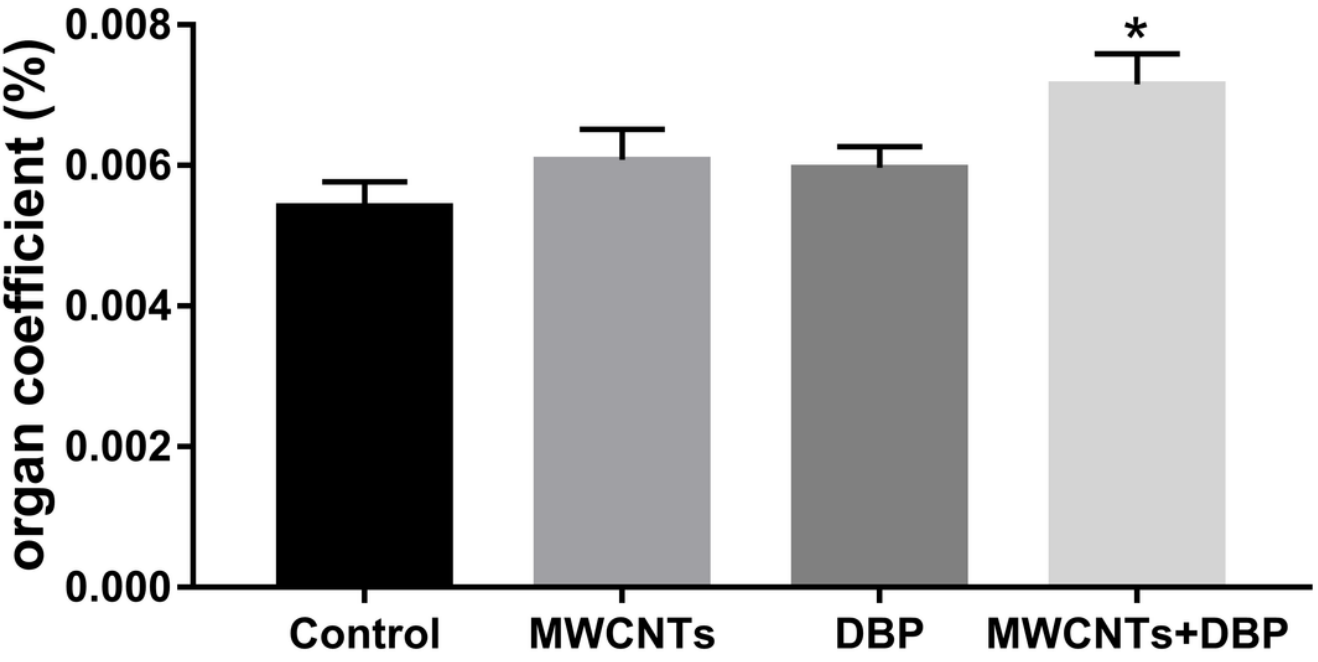

Figure 1

Lung organ coefficient of rats. The histogram values represent the Mean ± SEM (n = 10). * $p < 0.05$, ** $p < 0.01$.

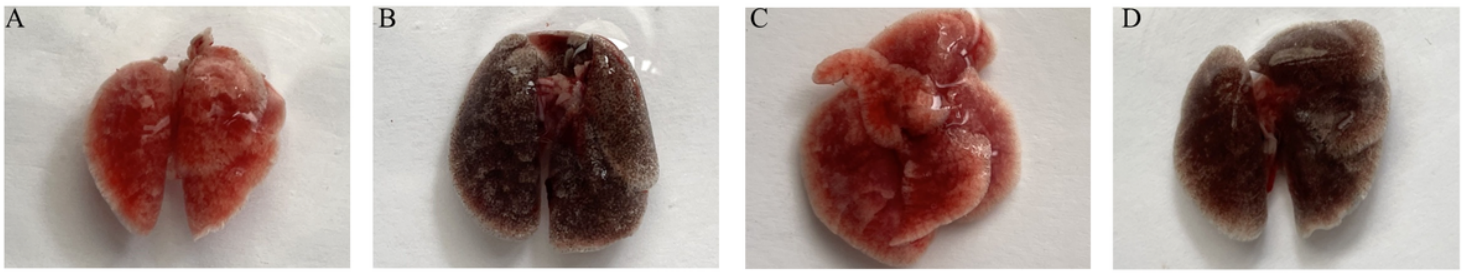

Figure 2

The crude appearance of the lung tissue. A: Saline control group; B: MWCNTs group; C: DBP group; D: MWCNTs+DBP combined exposure group.

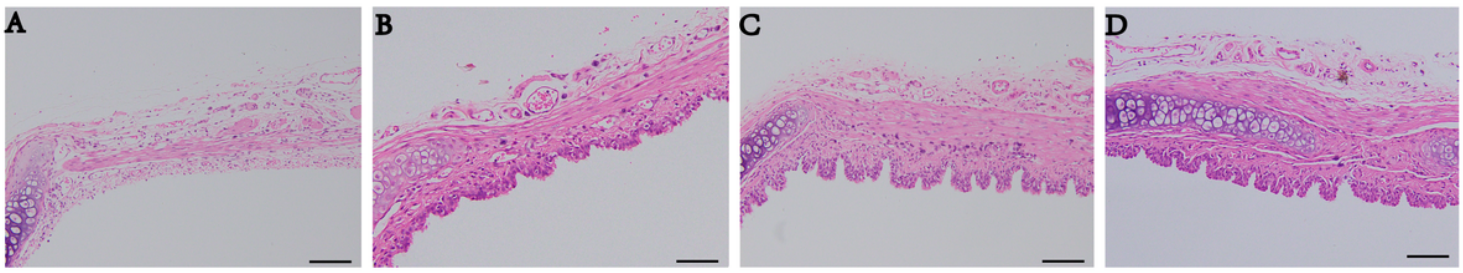

Figure 3

Results of tracheal H&E staining in rats, scale bar 100 um. A: Saline control group; B: MWCNTs group; C: DBP group; D: MWCNTs+DBP combined exposure group.

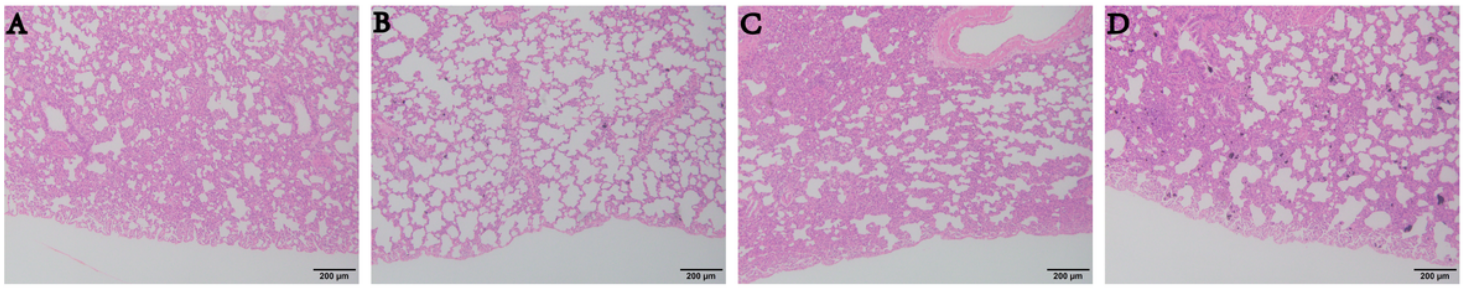

Figure 4

Results of H&E staining in rat lungs, scale bar 200 um. A: Saline control group; B: MWCNTs group; C: DBP group; D: MWCNTs+DBP combined exposure group.

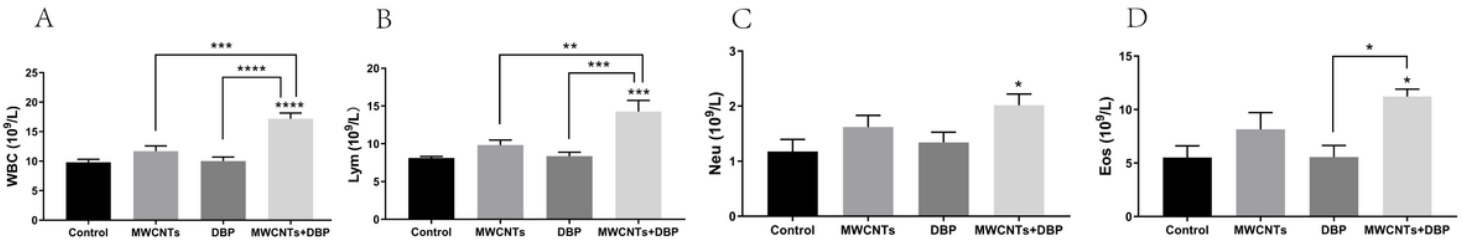

Figure 5

Cytology of BALF. A: Total number of leukocytes (WBC); B: Number of lymphocytes (Lym); C: Neutrophils (Neu); D: Eosinophils (Eos). The histogram values represent the Mean ± SEM (n = 10). * $p < 0.05$, ** $p < 0.01$.

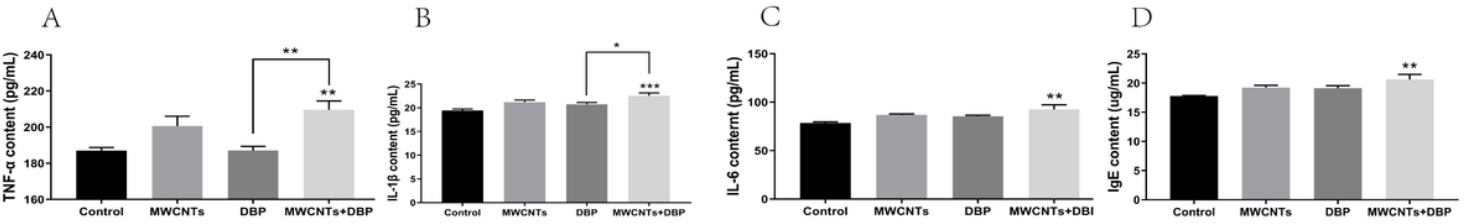

Figure 6

Biochemical analysis of BALF. A: Tumor necrosis factor α (TNF-α); B: Interleukin 1β (IL-1β); C: Interleukin 6 (IL-6) D: Immunoglobulin E (IgE). The histogram values represent the Mean ± SEM (n = 10). * $p < 0.05$, ** $p < 0.01$.

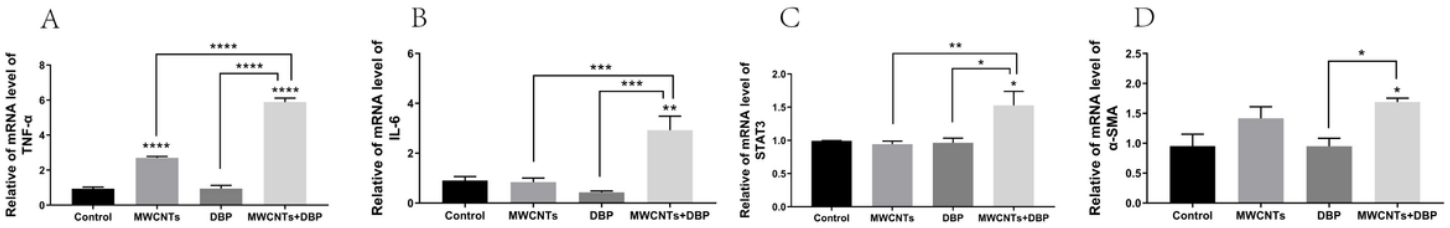

Figure 7

mRNA levels of airway inflammation marker genes in rats. A: TNF-α; B: IL-6 C: signal transduction and activating transcription factor 3 (STAT3); D: α-SMA. The histogram values represent the Mean ± SEM (n = 10). * P < 0.05, ** P < 0.01.

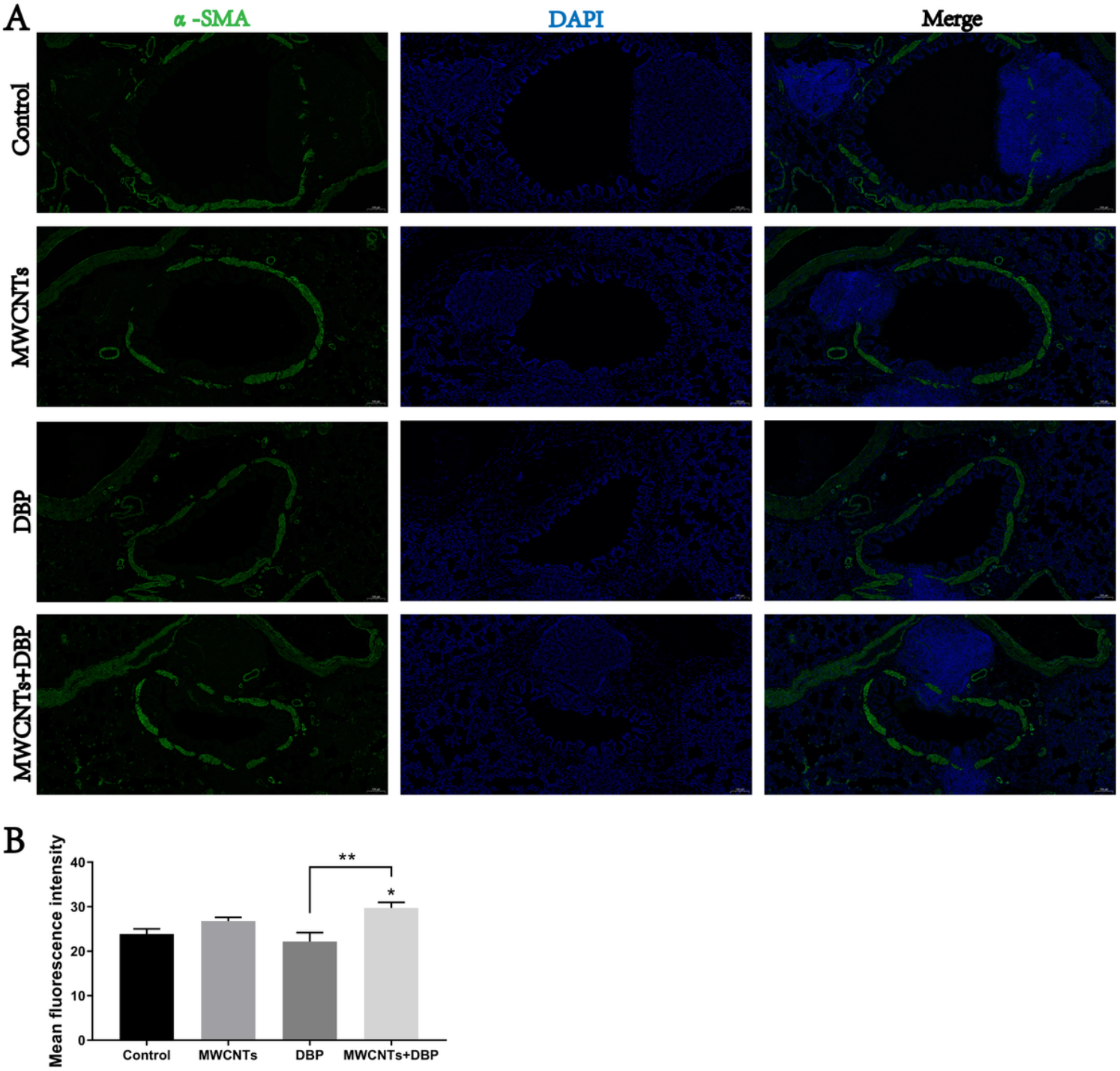

Figure 8

A: Representative images of bronchia after immunofluorescence staining, scale bar 100 um; B: Quantification of α-SMA expression levels. The histogram values represent the Mean ± SEM (n = 10). * $p < 0.05$, ** $p < 0.01$.

Supplementary Files

This is a list of supplementary files associated with this preprint. Click to download.

- FigureS1.pdf